SIN-CHN SCIENTIFIC PRESS PTE.LTD.

Molecular & Cellular Biomechanics 2025, 22(1), 987.
https://doi.org/10.62617/mcb987

Article

Biomechanical model study on the effect of floor materials on walking stability in tea space design

Bin Liu

College of Art and Design, Guangxi Vocational and Technical College, Nanning 530226, China; lb53302@163.com

CITATION

Liu B. Biomechanical model study on the effect of floor materials on walking stability in tea space design. Molecular & Cellular Biomechanics. 2025; 22(1): 987. https://doi.org/10.62617/mcb987

ARTICLE INFO

Received: 3 December 2024
Accepted: 12 December 2024
Available online: 3 January 2025

Abstract: Floor materials have a considerable impact on walking stability, especially in tea spaces where quiet and comfort are crucial. The materials used have an impact on users' biomechanics, which influences balance, postural stability, and overall enjoyment in these places. Despite their importance, few studies have looked into the biomechanical impacts of floor materials in such environments. The purpose of this research is to create a biomechanical model to assess the impact of various floor surfaces on walking stability in tea space design, with the use of artificial intelligence (AI) for prediction. A biomechanical model using AI algorithms was used to simulate walking movements on different floor materials. The model predicts walking stability using friction, surface texture, and material hardness. The data were acquired using motion capture and sensor technology; data from people walking on surfaces like wood, ceramic tiles, and tatami mats were obtained and pre-processed by data cleaning, and *z*-score normalization, extracting features using Principal Component Analysis (PCA). The trained data are processed using Dynamic Grasshopper Optimized Deep Belief Network (DGO-DBN) techniques to improve forecast accuracy. The results show that wooden and tatami surfaces are more stable than ceramic tiles, which have a higher risk of slips and trips. The findings highlight the necessity of appropriate material selection in tea space planning to improve walking stability and reduce safety issues. This research offers light on how biomechanical analysis, paired with AI, might influence better design decisions for spaces that promote user comfort and safety.

Keywords: floor materials; Dynamic Grasshopper Optimized Deep Belief Network (DGO-DBN); tea space design; walking stability

1. Introduction

Tea spaces, as the specific places where individuals take tea, comprise features that enhance the aesthetics or functionality of the space [1]. For example, movement such as the stability of individuals in restricted areas within such spaces is one determining factor concerning the safety of the spaces and the flow of traffic [2]. People's walking stability, which is their ability to walk safely and maintain balance, is affected by several factors, with the type of floor being among the most significant [3]. Floors vary in friction, cushioning and general outlook, which determines how conveniently and safely individuals maneuver their way around the floors. [4]. When deciding on the floor in the design of the tea space, the selection is not only a personal decision to choose noble materials for the floor but also functional, particularly in the areas where it is assumed that people will often move frequently, such as tea houses, tea rooms or tea gardens [5]. Being the internal surface and the largest area of the interior, the floor material should be chosen with the combination of beauty and such functional properties as safety for all people, including the disabled, ease of movement, and comfort for the inhabitants [6].

In tea spaces, this involves determining how the kind of floor affects wheelchair-bound persons, elders, or persons with any physical challenges [7]. Selection of flooring can determine how such individuals are able to move around the area, and their level of comfort and safety in the area [8]. Thus, the choice of the floor type that should be used in the construction of the tea space is not only based on the beauty of aesthetics but also stability throughout when walking as well. These factors can include friction, type of cushioning and relationship between sensory organs and designed Tea spaces so that any designed space is comfortable to all visitors [9]. It is necessary to evaluate floor coverings for walking stability since it demonstrates that it is possible to have better tea in safe and enjoyable conditions [10].

The purpose of this work is to create a biomechanical model to assess the impact of various floor surfaces on walking stability in tea space design, with the use of artificial intelligence (AI) for prediction.

Key contribution

- A dataset of motion capture and sensor technology data from people walking on surfaces like wood, ceramic tiles, and tatami mats was collected.
- Data preprocessing using data cleaning, and *Z*-score normalization to clean the data. PCA is employed for feature extraction, where high dimensionality is achieved by distinguishing the directions of variance so as to convey complex details in a simple approach.
- The DGO-DBNN, a technique to improve forecast accuracy of floor materials on walking stability in tea space design.

The remaining research is addressed in the sections that follow: Part 2 provides a summary of previous research. Part 3 presents the suggested method. Part 4 evaluates and explains the results of using the suggested approach. Part 5 describes the discussion of the research. Conclusion is shown in Part 6.

2. Related work

A demonstration of the configuration for recording patterns of walking using a capacitive biosensor floor that might identify the location and timing of foot touches on the floor was described in Hoffmann et al. [11]. Using the configuration, individuals walked throughout a biosensor floor in various modes, including dual-tasking, normal pace, and closed eyes, among many others. The classification task of identifying the walking mode exclusively from the floor sensor data was trained and assessed using RNN-LSTM units.

A softmax that could increase walking performance after a long standup was examined by Lu et al. [12] to determine whether an ML algorithm might objectively evaluate fatigue levels. By employing an anti-fatigue mat, the harmful effects of prolonged standing could be reduced compared to walking directly on the ground. When measuring fatigue, the ML method showed a moderate level of accuracy.

Employing physically demanding activities to identify the walking intervals that cause changes in walking patterns within and across individuals, Alharthi et al. [13] provided a more detailed understanding of the mechanism of walking variability.

Deep learning techniques were used to fuse sensors from distributed POF sensors for walking recognition. Because the GRF varied in continuous steps across a continuous area, the floor sensor system records spatiotemporal samples.

By combining deep learning-based statistics with self-powered tribo electric floor mats, Shi et al. [14] demonstrated a smart floor monitoring system. The floor mats were made with distinctive identity electrode patterns by a low-cost, highly adaptable printing method that allowed for parallel communication to lower the computational cost of deep learning and system complexity. The instantaneous sensory data processing might be used to determine the walking position, active status, and identity details.

A method to evaluate walking balance using inertial measurement units installed on wearable technology was presented by Lattanzi and Freschi [15]. The suggested method comprised the extraction of time-domain, frequency-domain, and structural elements that were suggested in a range of common petrographic evaluation techniques based on force plates. It was significant and the features showed notable ability in the identification of walking balance tasks.

To identify thirteen common human motions, including falls (the front, rear, right, and left), kneeling, downwards, ascending stairs, walking, bending both ways, and pushing a cart backward. Anderson et al. [16] introduced a P2S2 built-in shoe insole. The pressure that increased electrical signals in the different motions was recorded by placing six FSR detectors on key pressure locations on the insoles. The P2S2 was used to examine adult individuals in total. To provide the pressure data into many ML methods, such as k-NN, neural networks, and SVM algorithms. Four-fold cross-validation was used in the training of the ML models.

A structure- and sampling-adaptive method for determining footsteps GRF and walking balance symmetry by evaluating structural floor vibrations caused by human footsteps was examined [17]. Creating a balance between symmetry and footstep GRFs were important predictors of fall risk in the elderly and general walking health. Operational constraints prevent previous efforts, such as wearable sensing, computer vision, pressure sensors, and direct observation by qualified medical professionals.

The relationship between two clinical indicators for falling risk and walking stability was examined by Promsri et al. [18], displaying several movement elements or synergies together to achieve the walking task objective. The first five principal movements were then subjected to the biggest Lyapunov exponent (LyE), which was interpreted as a measure of stability. The higher the LyE, the less stable the individual movement components.

To investigate the variations in control of biomechanics posture during single-leg stance on a flat and textured stability board, as well as the lower extremity muscle activation during the same stance on the floor, a plain stability boardand a textured stabilityboard occured [19]. The experimental outcome demonstrated that healthy individuals prefer smooth-textured balancing boards.

Classifying laminate flooring choosing criteria from the perspectives of specialists was determined in Singer and Özşahin [20]. Experts assisted in determining the five primary criteria and twenty sub-criteria. A hierarchy with three levels was developed for comparison. Each criterion's significance was assessed using the spherical fuzzy algorithmic hierarchical approach. Because it helps to

analyze the important characteristics of laminate flooring, the suggested method offered an alternative perspective.

User stability was measured when using walking frames and determined if it was in compliance with walking frame usage guidelines. Furthermore, Thies et al. [21] investigated the opinions of healthcare experts and consumers on the usage of walking aids and instrumented walking frames, or Smart Walkers. Using Smart Walker's and pressure-sensing insoles, it examined how older adults used their homes; contextual data was recorded through corresponding video.

The ensemble-based empirical mode deconstruction (EEMD) approach would be used to better understand and identify the walking motions of people wearing exoskeletons, as investigated by Qiu and Liu [22]. Classification techniques utilized the internal mode functions (IMFs) that EEMD retrieved from the original walking signals as inputs.

The performance of a novel HC-CLT system under human-induced vibration was investigated in Huang et al. [23]. Three different kinds of HC-CLT floors, three-ply, five-ply, and five-ply with hollow cores in both the horizontal and transverse directions, were chosen as the subjects. Theoretical investigation revealed that HC-CLT floors had significant potential for fundamental applications and indicated the hollow cores had a minor effect on the statically bending stiffness.

The biomechanical modifications of the pelvic floor constitute by pelvic floor muscle training (PFMT), which aggravates the symptoms of stress urine incontinence (SUI) [24]. Strengthening muscle groups were significantly associated with symptoms of SUI. The experimental outcome demonstrated how PFMT improves the symptoms of stress urine incontinence.

A vision-based system was presented by Nouredanesh et al. [25] to automatically identify the most popular level flooring to better understand walk-related FLDBs and understand if surroundings affect elderly people's walking. Fallers and non-fallers utilized IMUs and some belt-mounted sensors to collect the unique datasets known as MAGFRA-W. The frames and image patches assigned and walking were annotated for indoor environments: high-friction components, wood, and tiles.

3. Methodology

Motion capture and sensor data were gathered from individuals walking on wooden, ceramic, and tatami floors. Preprocessing with data cleaning and *z*-score normalization, PCA was applied for feature extraction. A DGO-DBN model was developed to predict walking stability. Results showed that wooden and tatami floors offer greater stability than ceramic, highlighting the importance of floor material in tea space design and overall paper flow, as shown in **Figure 1**.

Figure 1. Overall paper flow.

3.1. Data collection

Data has been collected from Kaggle source [26]. This dataset contains biomechanical data collected from 100 participants walking on various floor materials (wood, ceramic tiles, and tatami mats) in the context of tea space design. This dataset was extremely important for biomechanical modeling that aids in the development of improved safety standards and recommendations for flooring selection in a variety of contexts. The impacts of various surfaces on posture mechanics, including motion capture data that would provide a more accurate analysis of walking patterns. The primary objective of this dataset is to assess and predict walking stability based on the physical properties of the floor materials, such as friction, surface texture, and material hardness, as well as the gait parameters of participants, including walking speed, step length, ground reaction forces, and sway velocities.

3.2. Data preprocessing

Data pre-processing can be divided into two phases, that is data cleaning and *z*-score normalization. Data preparation through which noise, outliers, or other observations must be excluded or corrected in the data set. Normalization is then done using *Z*-score to get an average of zero and a standard deviation of one for the variable. This process makes it possible to bring all factors to the same level to reduce the effect of a quantity on analysis results and improve the accurateness of model outcomes.

3.2.1. Data cleaning

Data cleaning for this dataset involves several steps to ensure the accuracy and consistency of the collected information. First, any missing or incomplete data points should be identified and handled, either by imputing values based on statistical methods or removing incomplete entries if necessary. Outliers and erroneous data, such as extreme values outside the expected range for walking parameters or floor material properties, should be detected and corrected or excluded. Finally, any

irrelevant or duplicate records should be removed to ensure that only relevant, unique data remains for analysis.

3.2.2. *Z*-score normalization

A raw data point that is above or below the group's mean is represented by the *Z*-score, a traditional standardization and normalization technique that counts the number of standard deviations. Ideally, it falls between −3 and +3. The dataset is normalized to the previously given scale, converting any data with different scales to the standard scale.

By subtracting the population mean from a raw data point and dividing it by the standard deviation, it was able to normalize the data through the *Z*-score. This resulted in a score that ideally varied between −3 and +3, indicating the number of standard deviations a value was above or below the mean, as determined from Equation (1), where w represented the value of a specific sample, μ the mean, and σ the standard deviation.

$$z_{score} = \frac{(w - \mu)}{\sigma} \tag{1}$$

3.3. Feature extraction

Principal Component Analysis (PCA) was employed to reduce the dimensionality of the data and classify the most significant issues affecting walking stability in tea space design. By analyzing variables such as floor texture, slipperiness, and material composition, PCA helped uncover patterns and relationships that are not immediately obvious in the raw data. The method helped to derive factors that characterized the variation in stability of the walking movements by providing better insights into how stability is affected by floor material.

PCA

A linear dimensionality reduction method called PCA projects the data in the direction using the greatest variation. Using this method, pertinent features are extracted through the data collection. As in Equation (2), $z_{(l)}$ represents the signal section. Where N represents the quantity of material samples. According to Equation (3), the materials $z_1, z_2, \ldots, z_M$ correspond to M observations of materials. The $N \times M$ matrix represents the complete ensemble of material.

$$z_{(l)} = \begin{bmatrix} z(1) \\ z(2) \\ \vdots \\ z(N) \end{bmatrix} \tag{2}$$

$$Z = [z_1, z_2, \ldots, z_M] \tag{3}$$

The following are the stages in the PCA: Find the vector's mean. Each material mean vector is determined using Equation (4).

$$\bar{z} = \frac{1}{N} \sum_{j=1}^{N} z_j \tag{4}$$

Determine the mean updated data in Equations (5) and (6):

$$yadi_j = z_j - \bar{z} \tag{5}$$

$$Yadi = [yadi_1 yadi_2 \ldots . yadi_M] \tag{6}$$

Determine the matrix of covariance in Equation (7):

$$D = \frac{1}{N-1}\sum_{k=1}^{N}\left(z_j - \bar{z}\right)^S (z_j - \bar{z}) \tag{7}$$

Determine the eigenvalues as well as eigenvectors of the matrix of covariance. Eigenvectors $f_j$and eigenvalues $\lambda_j$satisfy Equation (8).

$$D.f_j = \lambda_j \times f_j, \;\; j = 1, \ldots . M \tag{8}$$

Selecting elements and creating a feature vector. The largest-valued eigenvector is the main element. The elements are then returned of relevance after the eigenvectors are arranged from highest to lowest by eigen values. Therefore, using Equation (9), the quantity of variance,q_L for every eigenvalue is calculated.

$$q_L = \frac{\sum_{j=1}^{L}\lambda_j}{\sum_{j=1}^{M}\lambda_j} \tag{9}$$

Additionally, Equation (10) displays the principal component whose percentage of deviation is above the percentage criteria th, which is $0.9\ or\ 0.95$. The new data collection is derived. By using Equation (11), a final dataset is obtained.

$$\hat{q}_L = (q_L \geq th) \tag{10}$$

$$Zpca_{(l)} = \hat{q}_L^S Yadi^S \tag{11}$$

3.4. DGO-DBNN

The proposed DGO-DBN integrates the DGO with a DBN to predict walking stability on different floor materials in tea space design. The DGO adjusts the hyperparameters of the DBN in a dynamic form and enhances the consideration of the complex relationships between floor material properties, which include friction, surface texture, and hardness about walking stability. Using it in deep learning applications requiring fewer layers, the DBN is specifically optimized for real-time prediction systems and high accuracy. The model mimics walking dynamics on wooden floors, ceramic tiles, and tatami mats through recorded motion and sensor data. The enhancement of the network parameters used in the DGO-DBN brings better prediction of results to be strategic in planning for a better floor material choice as a sign of improved stability, which leads to the design of safe and more comfortable tea spaces to establish as shown in Algorithm 1.

Algorithm 1 DGO-DBN

```
import numpy as np
from sklearn.preprocessing import StandardScaler
from keras.models import Sequential
from keras.layers import Dense, Dropout
from keras.optimizers import Adam
def load_data():
    X_train, y_train, X_test, y_test = load_data_from_file()
    scaler = StandardScaler()
    X_train = scaler × fit_transform(X_train)
    X_test = scaler × transform(X_test)
    return X_train, y_train, X_test, y_test
def create_dbn_model(input_dim):
model = Sequential()
    model.add(Dense(512, input_dim = input_dim, activation = 'relu'))
    model.add(Dropout(0.2))
    model.add(Dense(256, activation = 'relu'))
    model.add(Dropout(0.2))
    model.add(Dense(128, activation = 'relu'))
    model.add(Dense(1, activation = 'sigmoid'))stability)
    model.compile(optimizer = Adam(), loss = 'binary_crossentropy', metrics = ['accuracy'])
    return model
def dynamic_grasshopper_optimization(dbn_model, X_train, y_train, num_grasshoppers = 30, max_iter =
100):
    grasshoppers = np.random.rand(num_grasshoppers, 3)
    best_position = None
    best_fitness = float('inf')
    for iteration in range(max_iter):
for i in range(num_grasshoppers):
        learning_rate = grasshoppers[i, 0]
        batch_size = int(grasshoppers[i, 1] × 64)
        neurons = int(grasshoppers[i, 2] × 512)
        model = create_dbn_model(X_train.shape[1])
        model.optimizer × lr = learning_rate
        model × fit(X_train, y_train, batch_size = batch_size, epochs = 10, verbose = 0)
        accuracy = model.evaluate(X_train, y_train, verbose = 0)[1]
        fitness = 1 − accuracy
if fitness < best_fitness:
            best_fitness = fitness
            best_position = grasshoppers[i, :]
      for i in range(num_grasshoppers):
grasshoppers[i, :] += np.random.rand(3) × (best_position − grasshoppers[i, :])
return best_position
def train_dgo_dbn(X_train, y_train, X_test, y_test):
best_hyperparameters = dynamic_grasshopper_optimization(None, X_train, y_train)
    learning_rate = best_hyperparameters[0]
    batch_size = int(best_hyperparameters[1] × 64)
    neurons = int(best_hyperparameters[2] × 512)
    model = create_dbn_model(X_train.shape[1])
    model × optimizer × lr = learning_rate
    model × fit(X_train, y_train, batch_size = batch_size, epochs = 50, verbose = 1)
    accuracy = model × evaluate(X_test, y_test)
    print(f'Test Accuracy: {accuracy[1] × 100:.2f}%')
if __name__ = "__main__":
    X_train, y_train, X_test, y_test = load_data()
    train_dgo_dbn(X_train, y_train, X_test, y_test)
```

3.4.1. DBN

A DBN is a generative model composed of multiple layers of stochastic networks for learning complicated features. Regarding walking stability in tea space design, DBNs could differentiate the effects of floor materiality on stability by recognizing the patterns. DBNs are methods of generative design. To obtain reliable performance in an unsupervised domain, a DBN consists of stacked Restricted Boltzmann Machines (RBM) that are trained greedily in layer-wise. A DBN is a set of RBM stages used for initial training that are subsequently further converted into a networks of forward feedback levels for weight adjusting using an alternate technique. Training is carried out in a DBN layer by layer, with each of the layers comprising an RBM trained over the previously trained layer by layer.

An approach known as greedy level-wise learning was used to develop a DBN level by level. The greed level-wise approach was used since it greedily advances every stage at a time. There is typically a fine-tuning phase following unsupervised training, during which a combined supervised training method is used for each layer. It combines two concepts: 1) that a deep neural network's initial parameter selection can have a major normalizing effect; 2) that understanding the input distribution can aid in understanding the mapping between inputs and outputs. A greedy level-wise unsupervised technique was used to train the underlying features in the pre-training phase, and enhance the features of the labeled models. DBN constitutes a type of deep learning architecture that combines multiple layers of unsupervised learning models. By stacking layers of RBMs, DBNs were primarily used to learn hierarchical representations of data that might be optimized for supervised learning tasks. **Figure 2** represents the architecture of the DBN.

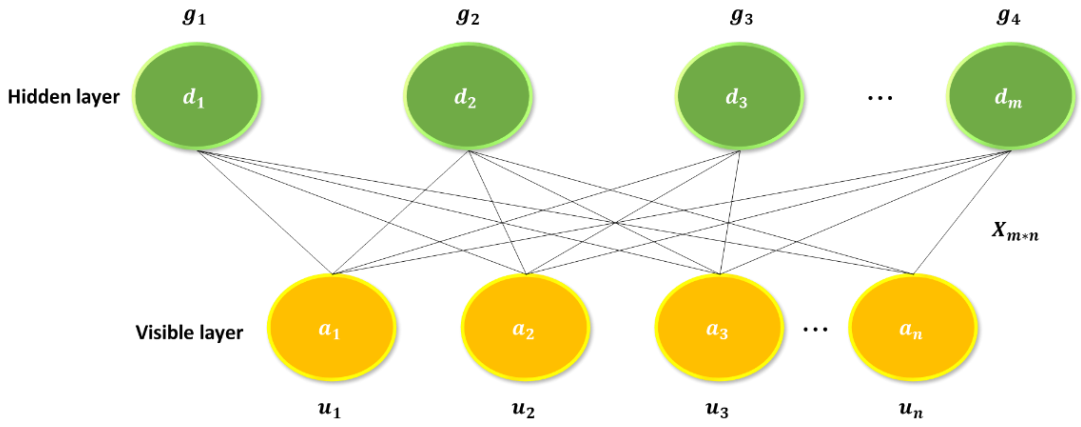

Figure 2. Architecture of DBN.

To illustrate the sophistication, it standardized the standard deviation, as shown in Equation (12).

$$\sigma^{\times} = \frac{\sigma - \sigma_{min}}{\sigma_{max} - \sigma_{min}} \tag{12}$$

Every visible unit in RBM is denoted by u, and every HL by g. To obtain the three parameters of the model, $\theta = \{X, B, A\}$ to determine the system. These were the visible layer component bias B, HL component bias A, and weight matrix X,

respectively. Assume that an RBM contains m visible cells and n hidden cells. The parameters structure is displayed as in Equation (13), with g_j denoting the i^{th} hidden unit and the j^{th} visible unit.

$$X = \{x_{j,i} \epsilon Q^{m \times n}\} \tag{13}$$

According to Equation (14), $x_{j,i}$ denotes the weight between the j^{th} visible cell and the i^{th} hidden cell. Where b_j stands for the bias thresholds of $the\ j^{th}$ visible cell (Equation (15)).

$$B = \{b_j \epsilon Q^n\} \tag{14}$$

$$B = \{a_i \epsilon Q^m\} \tag{15}$$

where a_i denotes the bias threshold for the i^{th} visible cell. Equation (16) represents the energy formula of RBM for a level of (u, g) through an actual situation, assuming that the hidden and visible layers follow the Bernoulli distribution.

$$F(u, g|\theta) = -\sum_{j=1}^{m} b_j u_j - \sum_{i=1}^{n} a_i g_i - \sum_{j=1}^{m} \sum_{i=1}^{n} u_j X_{ji} g_i \tag{16}$$

Here $\theta = \{X_{ji}, b_j, a_i\}$are the parameters of the RBM model, and the energy role presented the energy significance among the estimation of each node in the HL and each visible node. Equation (17) shows that the node set of layers that are visible and the node set of HLs were in a particular condition independently (u, g) to obtain the joint probability distribution equation, which was made possible by the normalization and exponential of the energy function.

$$O(u, g|\theta) = \frac{f^{-F(u,g|\theta)}}{Y(\theta)} \tag{17}$$

where $Y(\theta)$, a standard factor or distributive function that indicated the total energy coefficients of all possible conditions of the set of visible layers and hidden nodes, was identified in Equation (18).

$$Y(\theta) = \sum_{u,g} f^{-F(u,g|\theta)} \tag{18}$$

A common method for obtaining the parameters is to determine the probability function. It was possible to obtain the marginal distributions $O(u|\theta)$ of the nodes in the transparent layers by combining the overall circumstances of the HL nodes set in Equation (19) after presenting the joint likelihood distributions $O(u, g|\theta)$.

$$O(u|\theta) = \frac{1}{Y(\theta)} \sum_{g} f^{-F(u,g|\theta)} \tag{19}$$

In the visible stages, marginal distributions show the chance that the node's arrangement was inside the specific level range. The following important requirements are present in the RBM system due to its unusual layer-layer connections and inter-layer connectionless form: Every HL cell's enactment circumstances were restrictedly autonomous after the state of the accessible cells was

shown in Equation (20), which displayed the beginning likelihood of the i^{th} hidden element.

$$O(g_i = 1|u) = \sigma(a_i + \sum_j u_j X_{ji}) \tag{20}$$

Therefore, as shown in Equation (21), the beginning probability of the visible components was also conditionally independent after the condition of the concealed elements was defined.

$$O(u_j = 1|g) = \sigma(b_j + \sum_i X_{ji} g_j) \tag{21}$$

where the sigmoid function is denoted by $\sigma(w)$. Sorting out the three model parameters $\theta = \{X_{ji}, b_j, a_i\}$was crucial to choosing the RBM model. According to Equation (19), $O(u|\theta) = \frac{1}{Y(\theta)} \sum_g e^{-F(u,g|\theta)}$, power F is inversely related to probability O, and expanding O limits F, as shown by the following Equation (22), the inclination raise technique, which is related to the change of parameters that enhance the functional chance.

$$\theta = \theta + \mu \frac{\partial InO(u)}{\partial \theta} \tag{22}$$

This repetitive procedure decreased the energy F and increased the probability O. The algorithm's flow can be described as:

Step 1: Start the population and randomly generate a variety of concealed levels and the overall quantity of neurons in every stage.

Step 2: Determine the fitness rate using the routine technique and Equation (12), maintaining the ideal person in the present; overlap of intervals; and variance.

Step 3: Elite holds, retaining the person with the highest fitness value in the process progression.

Step 4: Determine whether the maximum number of repetitions has been reached. Once accomplished, either perform Steps 2 and 3 again or hold the network structures that are established.

Step 5: Train the system for floor detection using the best network architecture for DBN.

Step 6: Use the trained DBN model to classify the testing sets. Finally, compare the classification outcomes with the testing sets' classification data to confirm the accuracy of the classification.

3.4.2. DGO

The DGO method uses adaptive algorithms to quantify the effect of floor surfaces on stability during walking. By use of dynamic simulations, it adjusts design parameters and improves the layout of tea spaces to afford safety and convenience during movement by users. Natural grasshopper swarm behavior for resolving optimization issues. Equation (23) represents the mathematical model used to simulate the behavior of grasshopper swarms.

$$W_j = T_j + H_j + B_j \tag{23}$$

where W_j, T_j, H_j, and B_j stand for the jth grasshopper's position, social interaction, gravity force, and wind advection, respectively. Following implementing consideration of the randomness of the grasshoppers' positions, Equation (23) is expressed as follows:$W_j = q_1 T_j + q_2 H_j + q_3 B_j$, where $q_1, q_2, and\ q_3$ are at random in the interval $[0, 1]$, and T_j is defined by Equation (24).

$$T_j = \sum_{i=1, i \neq j}^{M} t(c_{ji}) \hat{c}_{ji} \tag{24}$$

The social force $t(q)$, where M is the number of hoppers in the swarm, $c_{ji} = |W_i - W_j|$ is the interval between the jth and ith grasshopper, and $\hat{c}_{ji} = \frac{W_i - W_j}{c_{ji}}$is the vector of units extending from the jth hopper to the ith grasshopper. Where f is the strength of the desire and k is the scale of attractive length, are denoted in Equation (25).

$$t(q) = ef^{-\frac{q}{k}} - f^{-q} \tag{25}$$

Let e represent the separation of two grasshoppers. The comfortable distance, c is the point at which two grasshoppers are not attracted to repulse by one another. Two grasshoppers are repelled by one another when c is less. The two grasshoppers are attracted to each other. Specifically, t rises as c shifts approximately. When c exceeds, t falls. t progresses to 0 and then does nothing. As a result, the distance between each of the grasshoppers is in the range of 1. As a result, the area between two grasshoppers is separated into three areas: the attraction, comfort, and repulsion zones, as shown in Equation (26).

$$H_j = -h\hat{f}_j \tag{26}$$

where $\hat{f}_j$ is a unity vector pointing toward the earth's center and h represents the gravitational constant, as shown in Equation (27).

$$B_j = v\hat{x}_j \tag{27}$$

where the wind direction is indicated by the unity vector $\hat{x}_j$ and the constant drift is v in Equation (28).

$$W_j = \sum_{i=1, i \neq j}^{M} t\left(|W_i - W_j|\right) \frac{W_i - W_j}{c_{ji}} - h\hat{f}_j + v\hat{x}_j \tag{28}$$

However, the swarm cannot converge at the designated spot after the grasshoppers have reached their comfort zone. Therefore, the optimization model cannot be simply solved using Equation (28). The optimization model is solved by modifying Equation (28) to Equation (29).

$$W_j^c = d \sum_{i=1, i \neq j}^{M} d \frac{va_c - ka_c}{2} t\left(|W_i^c - W_j^c|\right) \frac{W_i^c - W_j^c}{c_{ji}} + \hat{S}_c \tag{29}$$

where $\hat{S}_c$ is the cth element of the ideal grasshopper and va_c, ka_c are the upper and lower bounds of the cth element of the jth grasshoppers, respectively. The comfort, repulsion, and attraction zones can be reduced by decreasing the adaptive parameter $d, \hat{S}$. There is no H element in Equation (29) since the gravitational force is not taken under consideration. Additionally, assume that a target $\hat{S}_c$ is always in the following direction. To maintain equilibrium between the exploration and exploitation phases, the variable d is defined by Equation (30).

$$d = d_{max} - s\frac{d_{max} - d_{min}}{S} \tag{30}$$

where s indicates the current iteration S indicates the maximum iteration, and d_{max} and d_{min} represent the maximum and lowest of the variable d, respectively.

The newly updated location of the grasshopper is known as dynamic grasshopper optimization that can be calculated as follows in Equation (31) based on the influence of the gravity force that is not taken into consideration in the basic DGO: the accurate adjacent of Equation (29) reduced by the sum of the ratio between the gravity. Constant h and the vector of units through the jth grasshoppers to the ith grasshopper.

$$W_j^c = d\sum_{i=1, i\neq j}^{M} d\frac{va_c - ka_c}{2} t\left(\left|W_i^c - W_j^c\right|\right)\frac{W_i^c - W_j^c}{c_{ji}} - \sum_{i=1 i\neq j}^{M} h\frac{W_i^c - W_j^c}{c_{ji}} + \hat{S}_c \tag{31}$$

During hunting, the jth grasshopper's velocity updates its position in the process described below in Equations (32) and (33).

$$u_j^c = cv_j^c + b \times rand \times \left(\hat{S}_c - W_j^c\right) \tag{32}$$

$$W_j^c = W_j^c + u_j^c \tag{33}$$

where rand is a random number between $0\ and\ 1$ and b is the acceleration coefficient. As a result, the jth grasshopper uses the position's two updated methods, Equations (31) and (33). The location of the jth grasshopper is modified as follows in Equation (34) based on the chosen probability o.

$$W_j^c = \begin{cases} d\sum_{i=1, i\neq j}^{M} d\frac{va_c - ka_c}{2} t\left(\left|W_i^c - W_j^c\right|\right)\frac{W_i^c - W_j^c}{c_{ji}} - \sum_{i=1 i\neq j}^{M} h\frac{W_i^c - W_j^c}{c_{ji}} + S_c, o < 0.5 \\ W_j^c + cv_j^c + b \times rand \times \left(\hat{S}_c - W_j^c\right) \quad o \leq 0.5 \end{cases} \tag{34}$$

where d is identical to the basic GOA's value. The GOA is improved and written as DGO based on the above. The following are the specific actions that DGO requires:

Step 1: initialization, Set the initial values for the grasshopper swarms $W_j(j = 1,2, \ldots., M)$, d_{max}, d_{min}, the minimum and maximum velocities, and the maximum number of repetitions (S).

Step 2: Determine the ideal grasshopper $\widehat{S}$ by calculating each grasshopper's fitness. Assume $s = s + 1$.

Step 3: Use Equation (30) to update the value d.

Step 4: Involves mapping each grasshopper's distance from the others into the intervals $1,4$, and adopting the chosen probability, o. If o is less, Equation (31) or (34), respectively, are used to update the grasshopper's position. The grasshopper's position is updated using either Equation (34) or Equations (32) and (33) otherwise. The upper and lower bounds are used to update the grasshopper's position if it is found to be outside of the bound.

Step 5: Determine each grasshopper's fitness value. If a better grasshopper is available, update $\hat{S}$. Assume that $s = s + 1$.

Step 6: Determine if the terminal condition has been achieved. Return the ideal grasshopper$\hat{S}$if the answer is yes. If not, turn to step 3.

4. Result

Python 3.12 was operated on Windows 11 with an 11th-generation Core i7 processor and 32 GB of RAM. It made multitasking and development performance evaluations much easier due to this modern laptop design. The result demonstrates that the proposed DGO-DBN model can be used to optimize the floor material of tea space designs. There are three-floor materials that have been compared, such as wooden, tatami, and ceramic tiles.

4.1. Walking stability assessment based on floor material

Effects of floor types on several biomechanical properties. Analyzing these results through a DGO-DBN shows that tatami mats and wood are more effective than other materials. The ceramic tile floor's surface roughness is significantly lower at (35%), respectively, compared to Tatami (85%) and wooden (45%), thus providing a better grip as well as stability. Also, at 60% of material hardness, 85% of step length, and lower ground reaction force at 80%, Tatami and wood prove to have a good moderation of physical movements. According to the DGO-DBN model, the Tatami and wood are the most balanced options for biomechanical optimization, as shown in **Figure 3**.

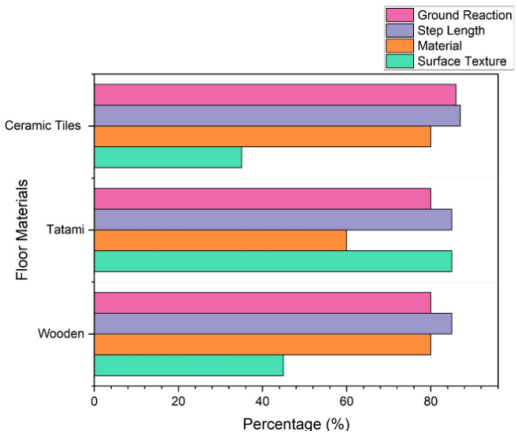

Figure 3. Walking stability assessment based on floor material.

4.2. Slip resistance

The important factor that mostly affects safety is the slip resistance of floor

materials, it minimizes chances of slips, falls and steadiness in diverse settings. The capacity of the surface to withstand slipping or sliding when pressure is applied, especially under damp or slick circumstances known as slip resistance. It was essential for reducing the risk of falls and injuries, particularly in moisture. The results further showed that wooden floors offered the highest slip resistance, with a value of 95%, followed by Tatami, with a value of 92%, and finally, the ceramic tiles, whose slip resistance value was 75%. These values indicate that wooden and tatami floors offer higher values of friction coefficient and thus reduce the tendency to slip than ceramic tiles. These differences show how flooring surfaces affect the stability of walking and overall tea space designs regarding user experience and protection. The DGO-DBN model can improve these design parameters for better results. **Figure 4** presents the result of slip resistance on floor materials.

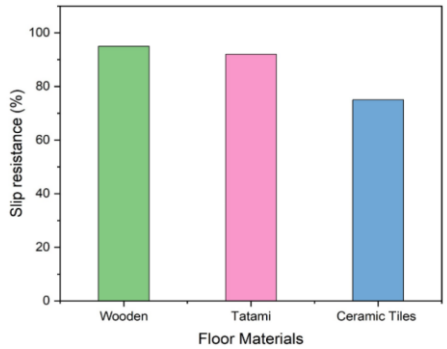

Figure 4. Result of slip resistance on floor materials.

4.3. Postural stability

Postural stability describes the ability of an individual to maintain an upright, balanced position, especially during movement on performing tasks. It determines the postural stability of floor materials where walking and other activities must be performed with stability and balance, as in tea space. With regard to the postural stability test, wooden floors have the highest results with 95%, Tatami carpet has 90% and ceramic tiles have 75%. These values imply that wooden and Tatami floors are more supportive and stable than ceramic tiles. Such differences are crucial for creating the most comfortable and safe tea zones for the end users. The DGO-DBN model can be used to optimize floor material choices to improve postural stability and overall user experience. **Figure 5** presents the result of postural stability on floor materials.

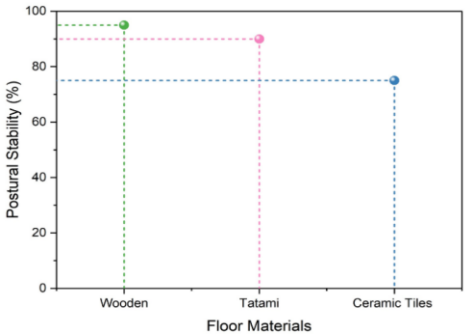

Figure 5. Result of postural stability on floor materials.

4.4. Muscle fatigue

The muscle fatigue caused by different floor materials is essential for evaluating walking comfort and stability in tea space design. The reduction in muscular force production known as muscle fatigue, and it usually happens after extended or vigorous physical exercise. Wooden floors result in the lowest muscle fatigue at 15%, followed by Tatami with 18%, and ceramic tiles, which cause the highest fatigue at 30%. Based on these findings, wooden and Tatami floors are preferred for walking over ceramic tiles because they reduce fatigue. The DGO-DBN model can be employed to optimize floor material selection, reducing muscle fatigue and enhancing user experience in tea spaces. **Figure 6** presents the result of muscle fatigue on floor materials.

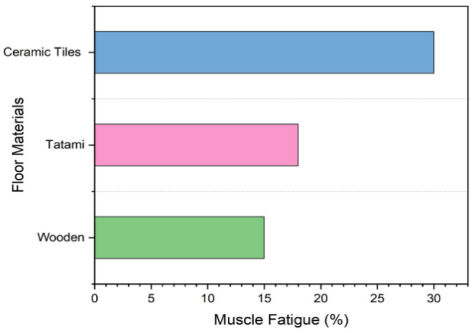

Figure 6. Result of muscle fatigue on floor materials.

4.5. Pressure distribution

Pressure distribution created by various floor materials is one of the main factors that affect walking stability and comfort in designing tea spaces. The pressure distribution describes how a load or force is delivered and how the pressure was distributed across a surface. Regarding flooring, it explains how an object's or person's weight was dispersed over the floor contact area. Wooden floors exhibit the highest pressure distribution at 95%, followed by tatami at 90%, and ceramic tiles at 85%. This suggests that wooden and tatami floors offer the most stability and comfort for walking, minimizing the risk of instability. The DGO-DBN model allows for achieving the optimal selection of floor material, which is also beneficial for improving walking stability in tea spaces and enhancing the overall user experience. **Figure 7** presents the result of pressure distribution on floor materials.

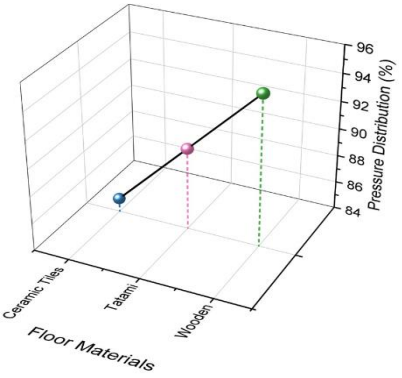

Figure 7. Result of pressure distribution on floor materials.

4.6. Comfort rating

Comfort ratings of floor materials influence user experience, stability, and comfort, with higher ratings offering better support. The subjective assessment of how physically pleasant a surface or substance feels after extended usage known as the comfort rating. Wooden floors, with a comfort rating of 90%, provide the highest level of comfort, followed by Tatami at 80%, and ceramic tiles at 50%. These ratings show that wooden and Tatami floors are more pleasant to walk compared to ceramic tiles, which can cause better stability and less fatigue. The DGO-DBN model can further improve the selection of floorings to increase stability while walking, and the satisfaction of the users within the tea space. **Figure 8** presents the result of the comfort rating on floor materials. **Table 1** illustrates the overall result parameters of floor materials.

Table 1. Overall result parameters of floor materials.

Floor Materials	Slip resistance (%)	Postural Stability (%)	Muscle Fatigue (%)	Pressure Distribution (%)	Comfort Rating (%)
Wooden	95%	95%	15%	95%	90%
Tatami	92%	90%	18%	90%	80%
Ceramic Tiles	75%	75%	30%	85%	50%

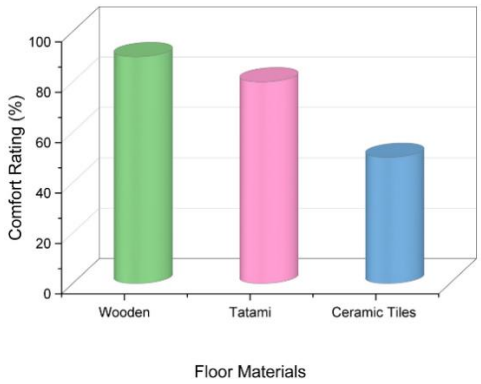

Figure 8. Result of comfort rating on floor materials.

5. Discussion

Wooden flooring offers high slip resistance but can yet pose a risk in wet situations, particularly in bathrooms. It provides good postural constancy, though it may lack grip for high-mobility activities like dancing or sports. Due to its lack of moderating effects, it might cause mild to moderate muscle tiredness while standing for extended periods of time. Comfort is generally high, but may not be ideal in colder surroundings. By maximizing stability and decreasing fatigue over time the suggested DGO-DBN model, which dynamically adjusts floor reactions on hardwood floors for postural stability. Tatami surfaces, while offering decent slip resistance, may be less reliable than wood during high-speed actions, increasing fall risk. Their postural constancy is slightly lower, potentially affecting balance during intense activities. With stronger mitigating, tatami can cause greater muscle fatigue over time and may not provide as much comfort or pressure distribution, especially for users with specific health situations. The DGO-DBN model helps to improve

stability by instantly adjusting the dynamics movement on tatami, which lessens fatigue and increases comfort levels. Ceramic tiles offer low slip resistance, especially in wet conditions, increasing the risk of chances. They provide less postural constancy, potentially causing balance issues in high-impact environments. Their resistance leads to muscle fatigue, making them inappropriate for continued standing. Furthermore, ceramic tiles do not distribute pressure effectively, resulting in discomfort for long-term standing or walking, earning the lowest comfort rating among materials. By improving postural stability and offering dynamic, real-time analysis of user's motions, the DGO-DBN model could assist in resolving problems. By enhancing postural stability, the suggested DGO-DBN model overcomes the issues with wooden and Tatami flooring. Through dynamic modeling and real-time analysis, DGO-DBN enhances stability by more accurately predicting and adapting to floor response, ensuring a smoother walking capability. The model optimizes the interaction between floor materials, reducing muscle fatigue and improving comfort compared to traditional testing methods.

6. Conclusion

The proposed biomechanical model, leveraging AI algorithms, offers a promising approach to evaluating the impact of floor materials on walking stability in tea spaces. Data collection involved acquiring walking movement data from individuals navigating various floor surfaces, including wood, ceramic tiles, and tatami mats, using motion capture and sensor technology. The collected data were then pre-processed through data cleaning and *Z*-score normalization to ensure consistency and eliminate noise. PCA was applied for feature extraction, allowing the identification of key factors affecting walking stability, such as slip resistance, postural stability, muscle fatigue, pressure distribution, and comfort. The proposed model, which employed DGO-DBN techniques, processed the pre-processed data to enhance forecast accuracy and predict the biomechanical effects of different floor surfaces on walking stability. The results demonstrated that wooden and tatami mat surfaces provided superior stability compared to ceramic tiles, with higher ratings in slip resistance (95%, 92%, and 75%), postural stability (95%, 90%, and 75%), muscle fatigue (15%, 18%, and 30%), pressure distribution (95%, 90%, and 85%), and comfort (90%, 80%, and 50%). These findings underscore the importance of selecting appropriate materials in tea space design to improve user comfort and safety. The use of a static dataset, which ignores individual variances and real-time fluctuations in walking behavior, is a limitation. Future research could address this by incorporating real-time motion data, exploring additional floor material types, and considering factors such as user age, physical condition, and other personal characteristics to enhance the model's accuracy and broader applicability.

Funding: This research was funded by the Guangxi Higher Education Young and Middle-aged Teachers' Scientific Research Basic Ability Enhancement Project (grant number 2024KY1037) and the Key Project of the 14th Five-Year Plan for Educational Science in Guangxi (grant number 2023ZJY1447).

Ethical approval: Not applicable.

Conflict of interest: The author declares no conflict of interest.

Abbreviations

RNN-LSTM	recurrent neural network based on Long Short-Term Memory
ML	machine-learning
POF	plastic optical fiber
GRF	ground reaction force
P2S2	plantar pressure sensor system
FSR	force sensitive resistors
K-NN	k-Nearest Neighbour
POMA-G	Gait Subscale of Performance-Oriented Mobility Assessment
HC-CLT	hollow-core cross-laminated timber
MAGFRA-W	Multimodal Ambulatory Gait and Fall Risk Assessment in the Wild
FLDBs	free-living digital biomarkers
IMUs	inertial measurement units
RBM	Restricted Boltzmann Machines
HL	hidden layer

References

1. Su, X. and Zhang, H., 2022. Tea drinking and the tastescapes of wellbeing in tourism.Tourism Geographies,24(6-7), pp.1061-1081.
2. Yoon, J., Lee, B., Chun, J., Son, B. and Kim, H., 2022. Investigation of the relationship between Ironworker's gait stability and different types of load carrying using wearable sensors.Advanced Engineering Informatics,51, p.101521.
3. Ni, S. and Ishii, K., 2023. The relationship between consumer behavior and subjective well-being in Chinese teahouses and cafes: A social capital perspective.Journal of Leisure Research,54(4), pp.429-452.
4. Xue, X., Wang, H., Xie, J., Gao, Z., Shen, J. and Yao, T., 2023. Two-dimensional biomechanical finite element modeling of the pelvic floor and prolapse.Biomechanics and Modeling in Mechanobiology,22(4), pp.1425-1446.
5. Trageser, N., Sauerwald, A., Ludwig, S., Malter, W., Wegmann, K., Karapanos, L., Radosa, J., Jansen, A.K. and Eichler, C., 2022. A biomechanical analysis of different meshes for reconstructions of the pelvic floor in the porcine model.Archives of Gynecology and Obstetrics, pp.1-9.
6. Uchida, T.K. and Delp, S.L., 2021.Biomechanics of movement: the science of sports, robotics, and rehabilitation. Mit Press.
7. Mashhouri, L., 2021. Applying safe flooring in housing environments related to the independent elderly: evaluating suitability flooring technology to absorb impact in the event of a fall.
8. Baobeid, A., Koç, M. and Al-Ghamdi, S.G., 2021. Walkability and its relationships with health, sustainability, and livability: elements of the physical environment and evaluation frameworks. Frontiers in Built Environment,7, p.721218.
9. Huang, Y., Yao, K., Zhang, Q., Huang, X., Chen, Z., Zhou, Y. and Yu, X., 2024. Bioelectronics for electrical stimulation: materials, devices and biomedical applications.Chemical Society Reviews.
10. Ding, Y., Pang, Z., Lan, K., Yao, Y., Panzarasa, G., Xu, L., Lo Ricco, M., Rammer, D.R., Zhu, J.Y., Hu, M. and Pan, X., 2022. Emerging engineered wood for building applications.Chemical Reviews,123(5), pp.1843-1888.
11. Hoffmann, R., Brodowski, H., Steinhage, A. and Grzegorzek, M., 2021. Detecting walking challenges in gait patterns using a capacitive sensor floor and recurrent neural networks.Sensors,21(4), p.1086.
12. Lu, Z., Sun, D., Xu, D., Li, X., Baker, J.S. and Gu, Y., 2021. Gait characteristics and fatigue profiles when standing on surfaces with different hardness: Gait analysis and machine learning algorithms.Biology,10(11), p.1083.
13. Alharthi, A.S., Casson, A.J. and Ozanyan, K.B., 2021. Spatiotemporal analysis by deep learning of gait signatures from floor sensors.IEEE Sensors Journal,21(15), pp.16904-16914.
14. Shi, Q., Zhang, Z., He, T., Sun, Z., Wang, B., Feng, Y., Shan, X., Salam, B. and Lee, C., 2020. Deep learning enabled smart mats as a scalable floor monitoring system.Nature communications,11(1), p.4609.

15. Lattanzi, E. and Freschi, V., 2020. Evaluation of human standing balance using wearable inertial sensors: a machine learning approach.Engineering Applications of Artificial Intelligence,94, p.103812.
16. Anderson, W., Choffin, Z., Jeong, N., Callihan, M., Jeong, S. and Sazonov, E., 2022. Empirical study on human movement classification using insole footwear sensor system and machine learning.Sensors,22(7), p.2743.
17. Fagert, J., Mirshekari, M., Pan, S., Lowes, L., Iammarino, M., Zhang, P. and Noh, H.Y., 2021. Structure-and sampling-adaptive gait balance symmetry estimation using footstep-induced structural floor vibrations.Journal of Engineering Mechanics, 147(2), p.04020151.
18. Promsri, A., Cholamjiak, P. and Federolf, P., 2023. Walking stability and risk of falls.Bioengineering,10(4), p.471.
19. Alfuth, M., Ebert, M., Klemp, J. and Knicker, A., 2021. Biomechanical analysis of single-leg stance using a textured balance board compared to a smooth balance board and the floor: A cross-sectional study.Gait & posture,84, pp.215-220.
20. Singer, H. and Özşahin, Ş., 2022. Prioritization of laminate flooring selection criteria from experts' perspectives: a spherical fuzzy AHP-based model.Architectural Engineering and Design Management,18(6), pp.911-926.
21. Thies, S.B., Bates, A., Costamagna, E., Kenney, L., Granat, M., Webb, J., Howard, D., Baker, R. and Dawes, H., 2020. Are older people putting themselves at risk when using their walking frames?.BMC geriatrics,20, pp.1-11.
22. Qiu, J. and Liu, H., 2021. Gait Recognition for Human-Exoskeleton System in Locomotion Based on Ensemble Empirical Mode Decomposition.Mathematical Problems in Engineering,2021(1), p.5039285.
23. Huang, H., Lin, X., Zhang, J., Wu, Z., Wang, C. and Wang, B.J., 2021, August. Performance of the hollow-core cross-laminated timber (HC-CLT) floor under human-induced vibration. InStructures(Vol. 32, pp. 1481-1491). Elsevier.
24. Rátonyi, D., Koroknai, E., Pákozdy, K., Sipos, A.G., Takacs, P., Krasznai, Z.T. and Kozma, B., 2024. The impact of short-term pelvic floor muscle training on the biomechanical parameters of the pelvic floor among patients with stress urinary incontinence: A pilot study.European Journal of Obstetrics & Gynecology and Reproductive Biology,302, pp.283-287.
25. Nouredanesh, M., Godfrey, A., Powell, D. and Tung, J., 2022. Egocentric vision-based detection of surfaces: towards context-aware free-living digital biomarkers for gait and fall risk assessment.Journal of neuroengineering and rehabilitation,19(1), p.79.
26. Ziya. Walking Stability Data on Various Floor Materials—Biomechanical Data for Analyzing Walking Stability.Available online: https://www.kaggle.com/datasets/ziya07/walking-stability-data-on-various-floor-materials (accessed on 2 November 2024).